Biophysical Chemistry 143 (2009) 79–84

Contents lists available at ScienceDirect

Biophysical Chemistry

journal homepage: http://www.elsevier.com/locate/biophyschem

The binding mode of porphyrins with cation side arms to $(TG_4T)4$ G-quadruplex: Spectroscopic evidence

Chunying Wei [a,*], Lihua Wang [a], Guoqing Jia [b], Jun Zhou [b], Gaoyi Han [a], Can Li [b,*]

[a] Key Laboratory of Chemical Biology and Molecular Engineering of Ministry of Education, Institute of Molecular Science, Shanxi University, Taiyuan 030006, China
[b] State Key Laboratory of Catalysis, Dalian Institute of Chemical Physics, Chinese Academy of Sciences, Dalian 116023, China

ARTICLE INFO

Article history:
Received 26 February 2009
Received in revised form 9 April 2009
Accepted 9 April 2009
Available online 16 April 2009

Keywords:
Binding modes
G-quadruplexes
Interaction
Porphyrin
Spectroscopy

ABSTRACT

Interactions of 5,10,15,20-Tetrakis(*N*-methylpyridinium-4-yl)-21*H*,23*H*-porphyrin (TMPyP4) and 5,10,15,20-Tetrakis(*N*-propylpyridinium-4-yl)-21*H*,23*H*-porphyrin (TPrPyP4) with the parallel four-stranded $(TG_4T)4$ G-quadruplex DNA in 100 mM K^+-containing buffer were studied using circular dichroism (CD) spectroscopy, visible absorption titration, and steady and time-resolved fluorescence spectroscopies. The results show that the binding stoichiometric ratios of both TMPyP4 and TPrPyP4 to $(TG_4T)4$ are 3:1. Two types of independent and nonequivalent binding sites with the higher and lower binding affinities are confirmed, and the stronger and weaker binding constants are 9.44×10^7 and 6.94×10^5 M^{-1} for $(TG_4T)4$–TMPyP4 complex, 7.86×10^7 and 6.35×10^5 M^{-1} for $(TG_4T)4$–TPrPyP4 complex, respectively. For both TMPyP4–$(TG_4T)4$ and TPrPyP4–$(TG_4T)4$ complexes, one porphyrin molecule stacks on the one end of G-quadruplex with the higher binding affinity, another two porphyrins bind weakly to the two external grooves. The size of cation side arms around porphyrin core almost fails to affect the binding mode, stoichiometry and affinity of porphyrin to $(TG_4T)4$ G-quadruplex in 100 mM K^+-containing buffer.

1. Introduction

G-quadruplex DNAs can inhibit the activity of telomerase in cancer cell and have drawn a considerable attention by acting as a promising anticancer drug targets [1–3]. The interactions of G-quadruplexes with porphyrin derivative 5,10,15,20-Tetrakis(*N*-methylpyridinium-4-yl)-21*H*,23*H*-porphyrin (TMPyP4) (Scheme 1A) have been extensively studied since TMPyP4 can inhibit the activity of telomerase upon binding to human telomeric G-quadruplex DNAs [4]. G-quadruplex DNAs contain multiple guanine quartets, which are planar arrangements of four Hoogsteen hydrogen-bonded guanines. The size of porphyrin ring is similar to that of guanine quartet, hence the stability of G-quadruplex DNA by porphyrin is due mainly to π–π stacking interaction between the porphyrin ring and guanine quartet.

Two main models have been proposed for binding of porphyrins to different types of G-quadruplexes in buffers containing K^+ or Na^+, namely, intercalative binding between adjacent G-quartets [5–7] and end-stacking on the G-quartet [7–10]. However, some other binding modes except π–π stacking interaction between the porphyrin ring and G-quartet have also been suggested. For example, S. Neidle, et al. recently reported an X-ray structure of a G-quadruplex-TMPyP4 complex [11], indicating that TMPyP4 molecules do not directly interact with G-tetrads in the G-quadruplex. In addition, the weaker external binding sites of porphyrin derivatives to different structures of G-quadruplexes were also observed very recently in several groups [12–16].

In our group we also observed two types of binding sites for complex of porphyrin derivative 5,10,15,20-Tetrakis(*N*-propylpyridinium-4-yl)-21*H*,23*H*-porphyrin (TPrPyP4) bearing *N*-propylpyridinium cationic side arms (Scheme 1B) with $(TG_4T)4$ in buffer containing Na^+ [17]. Recently, the interactions of both TMPyP4 and TPrPyP4 with human telomeric G-quadruplex $AG_3(T_2AG_3)_3$ also present a weaker external binding site and a stronger end-stacking binding site in buffer containing K^+ in the presence or absence of molecular crowding agent PEG [18].

As we know, the guanine-rich DNA sequence $(TTGGGG)n$ of the telomeric end in *Tetrahymena* can form the parallel four-stranded G-quadruplex structure in the presence of Na^+ and K^+ [19,20]. In our previous work we have studied the interactions of both TMPyP4 and TPrPyP4 with $(TG_4T)4$ G-quadruplex in 100 mM Na^+ buffer [7,17] and found that the size of cation side arms in porphyrin core will affect their binding interactions. But whether the binding interactions of both porphyrins with $(TG_4T)4$ in buffer containing K^+ is different are unclear. So here using circular dichroism (CD), visible absorption, and steady and time-resolved fluorescence spectroscopies, the binding stoichiometries, binding constants, and binding modes of

Abbreviations: TMPyP4, 5,10,15,20-Tetrakis(*N*-methylpyridinium-4-yl)-21*H*,23*H*-porphyrin; TPrPyP4, 5,10,15,20-Tetrakis(*N*-propylpyridinium-4-yl)-21*H*,23*H*-porphyrin; CD, circular dichroism.

* Corresponding authors. Tel.: +86 351 7010699, +86 411 84379070; fax: +86 351 7011022, +86 411 84694447.
E-mail addresses: weichuny@sxu.edu.cn (C. Wei), canli@dicp.ac.cn (C. Li).

0301-4622/$ – see front matter © 2009 Elsevier B.V. All rights reserved.
doi:10.1016/j.bpc.2009.04.005

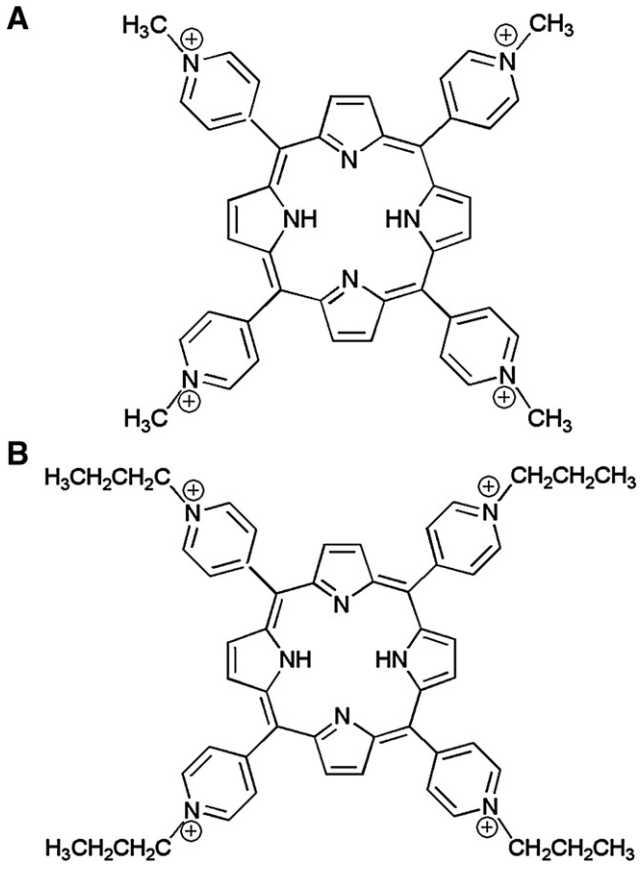

Scheme 1. The structures of TMPyP4 (A) and TPrPyP4 (B).

both TMPyP4 and TPrPyP4 to $(TG_4T)4$ G-quadruplex in 100 mM K^+-containing buffer (pH 7.5) were first studied in detail.

2. Materials and methods

2.1. Materials

The DNA oligonucleotide TG_4T was purchased from the SBS Genetech Co., Ltd. (China) in a PAGE-purified form, and TMPyP4 was purchased from Sigma-Aldrich. TPrPyP4 was synthesized according to our previous published procedure [17]. Single strand concentration of TG_4T was determined by measuring the absorbance at 260 nm at a high temperature using an extinction coefficient of 57,800 M^{-1} cm^{-1} [7]. The formation of G-quadruplex was carried out as follows: the oligonucleotide sample, dissolved in a buffer solution consisting of 10 mM Tris–HCl, 1 mM EDTA and 100 mM KCl at pH 7.5, was heated to 90 °C for 5 min, gently cooled to room temperature, and then incubated at 4 °C overnight. The concentrations of both TMPyP4 and TPrPyP4 were determined by measuring the absorbance at 424 and 423 nm with an extinction coefficient of 2.26×10^5 and 2.1×10^5 M^{-1} cm^{-1}, respectively [7,21].

2.2. Absorption spectroscopy

Absorption spectra were measured on a HP 8453 ChemStation with 1 cm-path-length quarter cell. Visible absorption titrations were terminated when the wavelength and intensity of the absorption band for porphyrin did not change any more upon three successive additions of G-quadruplex.

The titration data obtained were applied to construct the binding plots of r against C_f using Eqs. (1) and (2), where r is the moles of porphyrin bound to per mole of G-quadruplex, n is the numbers of equivalent binding sites, and K is the affinities of ligands for those sites [5,22]. The concentrations of free porphyrin (C_f) and bound porphyrin (C_b) were calculated using $C_f = C(1-\alpha)$ and $C_b = C - C_f$, respectively, where C is the total porphyrin concentration (3.5 μM). The fraction of bound porphyrin (α) was calculated using the equation, $\alpha = (A_f - A)/(A_f - A_b)$ [7,23], where A_f and A_b are the absorbance of the free and fully bound porphyrin at the Soret maximum of porphyrin, respectively, and A is the absorbance at the Soret maximum of porphyrin at any given point during the titration.

$$\frac{r}{C_f} = nK - Kr \tag{1}$$

$$r = \frac{n_1 K_1 C_f}{1 + K_1 C_f} + \frac{n_2 K_2 C_f}{1 + K_2 C_f}. \tag{2}$$

Eq. (1) is the Scatchard plot, and the plot of r/C_f versus r gives a linear curve when there is only one type of binding. If there are two types of binding sites, and each binding site does not influence the bindings on the other sites (noncooperative binding), Scatchard analysis can be expressed in Eq. (2), from which the number of each binding site (n_1 and n_2) and their binding constants (K_1 and K_2) can be obtained by nonlinear regression. Nonlinear regression analysis of the data was performed in the software of Origin 7.0 and errors were given as standard deviation obtained from the fits.

The percent hypochromicity of the Soret band of porphyrin can be calculated using hypochromicity % $= [(\varepsilon_f - \varepsilon_b)/\varepsilon_f] \times 100$, where $\varepsilon_b = A_b / C_b$ [9].

2.3. CD spectroscopy

CD experiments were performed at room temperature using a dualbeam DSM 1000 CD spectropolarimeter. Each measurement was the average of five repeated scans recorded from 220 to 320 nm in a 1 cm-path length quartz cell. The scanning rate (nm/min) was automatically selected by the Olis software as a function of the signal intensity to optimize data collection, and the data was obtained with a 1 nm bandwidth. The concentration of G-quadruplex is 10 μM. The scan of the buffer alone was subtracted from the average scan for each sample.

2.4. Steady and time-resolved fluorescence spectroscopies

Steady and time-resolved fluorescence measurements were performed using FL920 fluorescence lifetime spectrometer (Edinburgh Instruments, Livingston, UK) operating in the time-correlated single photon counting (TCSPC) mode. Excitation wavelength is set at 430 nm, and the slit width is 3 nm for both excitation and emission for steady fluorescence experiment. The samples were excited by 406.8 nm picosecond pulsed diode laser with pulse width 64.2 ps for time-resolved fluorescence measurement. All decay traces were measured using 4096-channel analyzer. The time resolution per channel was 24 ps. The number of peak counts was approximately 7000. For data analysis commercial software by Edinburgh Instruments was used. The data were fitted using a reconvolution method of the instrument response function (IRF) producing χ^2 fitting values of 1–1.3, and errors were given as standard deviation obtained from the fits. All these measurements were carried out three times to check the reproducibility and to obtain the average values for the lifetimes.

3. Results and discussion

3.1. Structural characterization of G-quadruplex DNA

CD has been used to examine the structures of quadruplex DNAs [24]. In order to get the exact information on the structure of

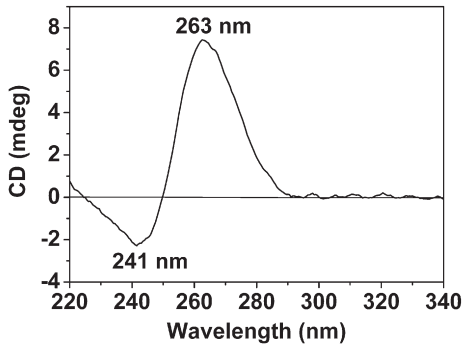

Fig. 1. CD spectra of 10 μM (TG_4T)4 G-quadruplex in buffer solution containing 10 mM Tris–HCl (pH 7.5), 1 mM EDTA, and 100 mM K^+.

TG_4T in K^+ buffer, the structure was characterized by CD spectra (Fig. 1). CD spectrum of TG_4T presents the positive and negative peaks near 260 and 240 nm, respectively, which is the typical parallel-stranded tetramolecular (TG_4T)4 G-quadruplex [25].

3.2. Binding stoichiometries and binding constants of porphyrins to G-quadruplex

To investigate the binding behaviors of both TMPyP4 and TPrPyP4 to (TG_4T)4 G-quadruplex, we first measured the visible absorption titration spectra of porphyrins by addition of the different concentrations of G-quadruplex (Fig. 2A, B). In the case of TMPyP4, the results show 10 nm red shift and 50% hypochromicity at the Soret band of TMPyP4 at the end of titration (the concentration of (TG_4T)4 G-quadruplex is 2.7 μM), whereas the red shift and hypochromicity at the Soret band of TPrPyP4 are 9 nm and 50% at the end of titration (the concentration of (TG_4T)4 G-quadruplex is 2.9 μM), respectively. Therefore, there is almost no difference for absorption spectra between TMPyP4–(TG_4T)4 and TPrPyP4–(TG_4T)4 complexes. Furthermore, the deviations from the isosbestic point were observed for both

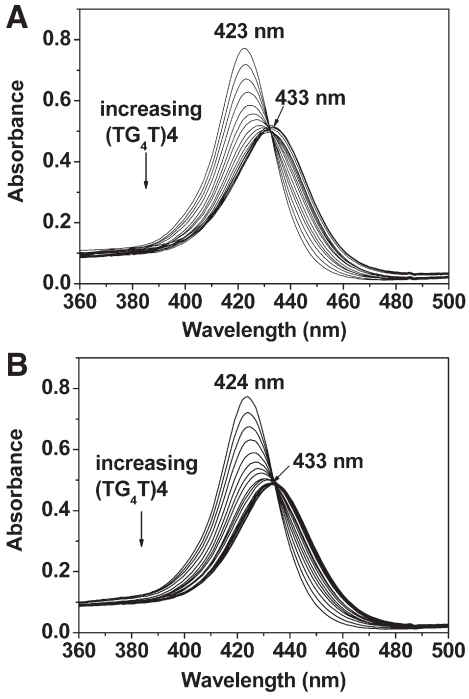

Fig. 2. Absorption titration of 3.5 μM TMPyP4 (A) or TPrPyP4 (B) with (TG_4T)4 G-quadruplex in the presence of 100 mM KCl. The concentration of (TG_4T)4 is 2.7 and 2.9 μM at the end of titration for TMPyP4 and TPrPyP4, respectively. All spectra were measured in 10 mM Tris–HCl (pH 7.5) and 1 mM EDTA buffer solution.

Table 1
The binding stoichiometries (n_1, n_2) and binding constants (K_1, K_2) of porphyrins to G-quadruplex in buffer solution containing 100 mM K^+.

Complexes	n_1	K_1 (M^{-1})	n_2	K_2 (M^{-1})
(TG_4T)4–TMPyP4	1.23 ± 0.05	$(9.44 \pm 0.18) \times 10^7$	1.75 ± 0.05	$(6.94 \pm 0.05) \times 10^5$
(TG_4T)4–TPrPyP4	1.23 ± 0.03	$(7.86 \pm 0.70) \times 10^7$	2.00 ± 0.06	$(6.35 \pm 0.04) \times 10^5$

porphyrins at the end of titration, which suggests that the binding of porphyrins to (TG_4T)4 should be composed of several steps, that is, there is more than one binding site.

Furthermore, the change in the maximum absorbance (423 and 424 nm) in the absorption spectra of TMPyP4 and TPrPyP4 was used to construct the Scatchard plots using Eq. (1). The Scatchard plots obtained are all nonlinear and upwardly concave (Fig. S1), which suggests that there are more than one type of binding site for TMPyP4 and TPrPyP4 in G-quadruplex, or that there are neighbor exclusion effects between two ligands. Scatchard plots are linear only for ligands binding to independent and equivalent sites [26].

To decipher whether curvature in Scatchard plot is due to several types of binding sites or due to neighbor exclusion effects, data are analyzed using Eq. (2) and the fit results are summarized in Table 1. The good fit results obtained by Eq. (2) (Fig. S2) indicate that there are two types of binding sites in the presence of K^+, and one binding does not influence the binding on another site. Interestingly, a recent crystal structure reported by S. Neidle et al. also observed two independent binding sites for TMPyP4 in the complex with human telomeric G-quadruplex DNA [11].

According to the fitting results, the binding constants for first (K_1) and second sites (K_2) of TMPyP4 are 9.44×10^7 and 6.94×10^5 M^{-1}, whereas the binding affinities for first (K_1) and second sites (K_2) of TPrPyP4 are 7.86×10^7 and 6.35×10^5 M^{-1}. So the binding affinities of both TMPyP4 and TPrPyP4 to (TG_4T)4 are almost the same. The binding stoichiometries of the first and second sites are 1.23 and 1.75 for (TG_4T)4–TMPyP4, respectively, while they are 1.23 and 2.00 for (TG_4T)4–TPrPyP4 complexes, respectively. That is, the stoichiometries of the first and second binding interactions for both complexes were

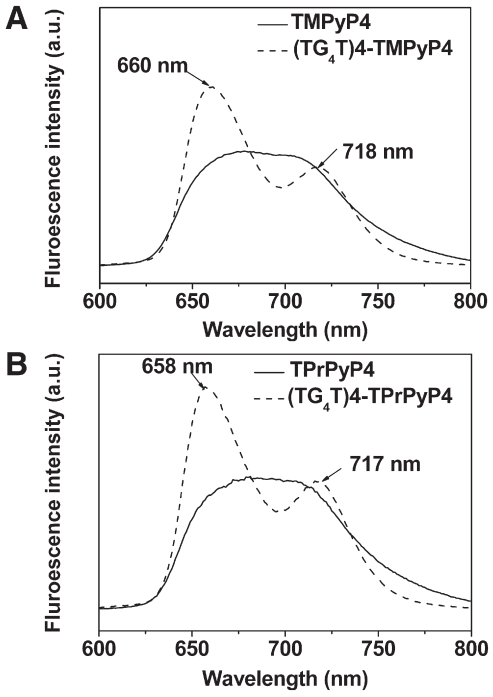

Fig. 3. Steady-state fluorescence spectra of 4.0 μM free porphyrins and G-quadruplex-porphyrin complexes (G-quadruplex/porphyrin = 2:1) in buffer solution containing 10 mM Tris–HCl (pH 7.5), 1 mM EDTA, and 100 mM K^+.

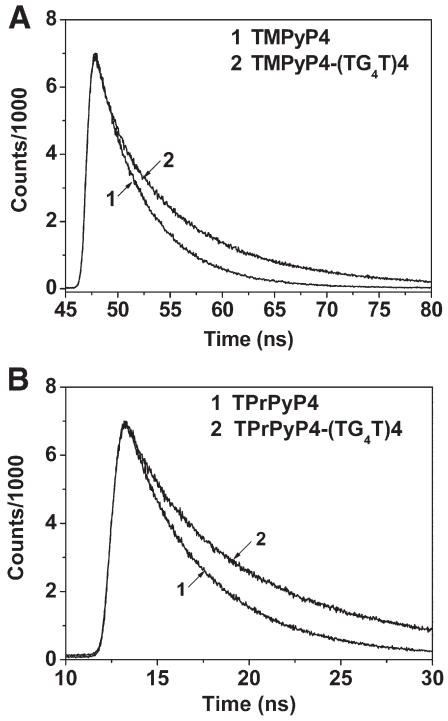

Fig. 4. Fluorescence decay curves of 4.0 μM free porphyrins and G-quadruplex-porphyrin complexes (G-quadruplex/porphyrin = 2:1) in buffer solution containing 10 mM Tris–HCl (pH 7.5), 1 mM EDTA, and 100 mM K^+.

found to be 1 and 2, respectively. Interestingly, very recently a low-affinity binding mode was detected at stoichiometry greater than 1 [18].

In addition, the binding affinities of both TMPyP4 and TPrPyP4 to site 1 (K_1) are about two orders of magnitude larger than to site 2 (K_2). This is consistent with the previous reports wherein porphyrin binding was indicated to present one secondary site with lower affinity [12,13]. More recently, the binding constants of some derivatives of porphyrin to *c-myc*, *c-kit* and telomeric G-quadruplexes have been determined, indicating that there are one higher and one lower affinity sites [14–18].

The current results about the binding stoichometries of TMPyP4 and TPrPyP4 with $(TG_4T)4$ G-quadruplex in K^+-containing buffer are different from our previous results in Na^+-containing buffer [9,17], in which the binding stoichiometry of TMPyP4 to $(TG_4T)4$ is 2 and the significant cooperative effect was observed, whereas the respective binding stoichiometries of TPrPyP4 for the stronger and weaker affinity sites are 1. This comparison revealed that the binding behaviors of porphyrins for G-quadruplexes are modulated by the nature of cation in buffer. Some controversies were also reported about effects of K^+ and Na^+ on the binding stoichiometries, exact modes, and binding sites of TMPyP4 to G-quadruplexes [5–10]. In addition, the size of the peripheral groups around porphyrin core fails to affect the binding stoichiometry and affinity of porphyrin to $(TG_4T)4$ G-quadruplex in buffer containing K^+.

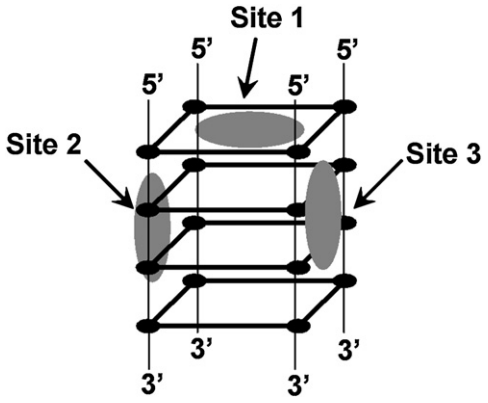

Scheme 2. Folding topology of parallel G-quadruplex along with the proposed binding sites of porphyrins. TMPyP4 and TPrPyP4 are shown in gray ellipses.

3.3. Binding modes of porphyrins to G-quadruplex

On the basis of absorption titration experiment, the values of hypochromicity % of both porphyrins are in the range of an intercalative binding (>35%), whereas the red shift values are slightly smaller than those of the typical intercalation (>15 nm). In fact, the red shifts (>15 nm) and hypochromicities (>35%) given for intercalative binding modes were determined for long pieces of duplex DNA [27], where the end-stacking is not significant. So the red shift value and hypochromicity associated with the binding stoichiometry and association constant suggest that porphyrins interact with G-quadruplex via stacking on G-quartet and outside binding.

In order to provide further insight into the binding sites of porphyrins for G-quadruplex, the steady and time-resolved fluorescence spectra were measured, which give the more detailed information of environment around a fluorophore [28]. Upon formation of complexes of porphyrins with G-quadruplex at a G-quadruplex/porphyrin molar ratio of 2, the featureless broad bands of porphyrins are split in two peaks near 660 and 720 nm, and the ratio of intensity at 660 nm to that at 720 nm is also increased significantly (Fig. 3).

The featureless emission spectra of porphyrins are due to coupling the first excited state S_1 with a nearby charge transfer state CT from the porphyrin core to pyridinium group [29]. Coupling is facilitated in high polarity solvents and by a high degree of rotational freedom of groups. The split of the $Q(0,0)$ and $Q(0,1)$ bands upon binding of porphyrins to DNA indicates that the electronic S_1–CT mixing within the bound excited molecule is less effective owing to a low polarity environment and confinement of porphyrin within binding sites, thus hindering free rotation of pyridinium groups.

It was reported that the outside bindings of TMPyP4 to both poly (dAdT)poly(dAdT) and RNA result in a split and significant increase in the intensity of the emission spectrum of TMPyP4 [30,31]. The peak positions and intensity ratios of $Q(0,0)$ to $Q(0,1)$ are in good agreement with our present results. It is worthy of noting that the fluorescence spectra of TMPyP4 in its complexes with $[poly\ (dG\text{-}dC)]_2$ and $[d(TACGTA)]_2$ are close to those obtained for $[poly(dA\text{-}dT)]_2$ [32], but an increasing ratio of $Q(0,0)$ to $Q(0,1)$ peak intensities and red

Table 2
The fluorescence lifetimes of porphyrins in the presence or absence of G-quadruplex in buffer solution containing 100 mM K^+.

Compounds	τ_1 (ns)	τ_2 (ns)	τ_3 (ns)
TMPyP4	1.94 ± 0.04 (15.11 ± 0.11%)	4.95 ± 0.02 (84.89 ± 0.16%)	0
$(TG_4T)4$–TMPyP4	1.33 ± 0.03 (6.31 ± 0.11%)	4.85 ± 0.03 (32.20 ± 0.21%)	10.89 ± 0.05 (61.48 ± 0.09%)
TPrPyP4	1.62 ± 0.08 (9.12 ± 0.39%)	4.67 ± 0.01 (90.88 ± 0.39%)	0
$(TG_4T)4$–TprPyP4	1.07 ± 0.02 (3.88 ± 0.02%)	5.53 ± 0.03 (25.46 ± 0.31%)	11.8 ± 0.03 (70.66 ± 0.32%)

τ values denote the fluorescence lifetimes that were obtained at 674 nm for free TMPyP4 and TPrPyP4, 658 nm for $(TG_4T)4$–TPrPyP4 complex, and 660 nm for $(TG_4T)4$–TMPyP4 complex. The data in bracket are the respective fractional amplitudes.

shifts of both peaks were observed in the order of [poly (dG-dC)]$_2$< [d(TACGTA)]$_2$<[poly(dA-dT)]$_2$, which was explained by an increase of the proportion of externally bound porphyrins at the expense of intercalated ones. So these results further indicate that both porphyrins interact with G-quadruplex by outside binding and the end-stacking on G-quartet.

Fig. 4 shows the fluorescence decays of porphyrins at 4 μM in the free form and complexes at 2:1 molar ratio of G-quadruplex to porphyrin, and their lifetime values are summarized in Table 2. According to the absorbance titration experiment, porphyrin molecules should be fully bound at 2:1 molar ratio of G-quadruplex to porphyrin. For free TMPyP4 and TPrPyP4 the fluorescence decays are biexponential, which consist with the reported results, wherein the biexponential fluorescence decay of TMPyP4 was attributed to the presence of two types of porphyrins: one is in solution and another is the adsorbed molecules on the surface of the quartz cuvette [33]. Here the shorter lifetimes at 1.94 and 1.62 ns with the fractional amplitudes of about 10% originate from the adsorbed porphyrins, and the longer lifetimes at 4.95 ns and 4.67 ns with the fractional amplitudes of about 90% are due to porphyrins in solution.

However the fluorescence decays for G-quadruplex-porphyrin complexes are triexponential. Except the shorter lifetime about 1 ns (only 3–6%) which is still ascribed to the adsorbed porphyrin on the surface of the quartz cell, there are another two longer lifetimes, which can be explained by two different localizations of porphyrin molecules within the G-quadruplex DNA. Two lifetimes of porphyrins further support the existence of two types of binding sites obtained by absorption titration fit.

It was reported that the lifetimes of TMPyP4 molecules bound in duplex DNA are about 10 and 1.5 ns [34–37]. But assignments of both lifetimes to the intercalated or the externally bound porphyrins are inconsistent. Shen et al. [34] and Liu et al. [36] suggested that the shorter lifetime is the externally bound porphyrin, and the longer lifetime is the intercalated porphyrin, whereas the opposite viewpoint was suggested by Csík et al. [35] and Turpin et al. [37]. In addition, in the case of TMPyP4-[poly(dG-dC)]$_2$ complex, the decay kinetics is found to be biexponential and the lifetimes are 2.5 and 7.0 ns, which are markedly shorter than those of the complexes with [poly(dA-dT)$_2$ (12 ns) [37]. It was found that the most probable types of interactions of porphyrin with [poly(dG-dC)]$_2$ and [poly (dA-dT)]$_2$ are the stacking on base pair (containing intercalation and end-stacking) and external binding, respectively. For TMPyP4-[poly(dG-dC)]$_2$ complex the shorter lifetime of 2.5 ns is attributed to intercalative porphyrin because adjacent G bases quench the fluorescence of porphyrin, whereas the longer lifetime of 7.0 ns is due to porphyrin by the end-stacking binding. Taking these results into account, we identify the shorter lifetimes about 5 ns as belonging to the end-stacking species and the longer lifetimes about 11 ns as belonging to externally bound porphyrin molecules in the grooves.

Because parallel-stranded (TG_4T)4 G-quadruplex has four identical grooves [38], according to the binding type, binding stoichiometry, binding affinity, and fluorescence lifetime of porphyrin to (TG_4T)4 G-quadruplex, we conclude that the stronger binding affinity of both TMPyP4 and TPrPyP4 to (TG_4T)4 is due to the end-stacking at site 1, whereas the external binding at sites 2 and 3 contributes to the second weaker binding mode (Scheme 2).

4. Conclusions

In summary, two types of independent and nonequivalent binding sites for both TMPyP4 and TPrPyP4 to parallel G-quadruplex (TG_4T)4 in the presence of 100 mM K^+ were confirmed, and the stronger and weaker binding affinities are 9.44×10^7 and 6.94×10^5 M^{-1} for (TG_4T)4–TMPyP4 complex, 7.86×10^7 and 6.35×10^5 M^{-1} for (TG_4T)4–TPrPyP4 complex, respectively. One porphyrin molecule stacks on the one end of G-quadruplex with the stronger binding affinity, and another two porphyrin molecules bind to the two external grooves by the weaker binding interaction. Obviously, the effect of the cation side arms *N*-methylpyridinium and *N*-propylpyridinium in porphyrin core on interactions of porphyrins with (TG_4T)4 is insignificant in K^+ buffer.

Acknowledgements

This work was supported by the National Natural Science Foundation of China (20503029, 20673110), Natural Science Fund of Shanxi Province (2009011012-2) and the Scientific Research Foundation for the Returned Overseas Chinese Scholars of Shanxi Province (2007).

Appendix A. Supplementary data

Supplementary data associated with this article can be found, in the online version, at doi:10.1016/j.bpc.2009.04.005.

References

[1] W.D. Wilson, H. Sugiyama, First international meeting on quadruplex DNA, ACS Chem. Biol. 9 (2007) 589–594.
[2] E.M. Rezler, D.J. Bearss, L.H. Hurley, Telomeres and telomerase as drug targets, Curr. Opin. Pharmacol. 2 (2002) 415–423.
[3] L. Oganesian, T.M. Bryan, Physiological relevance of telomeric G-quadruplex formation: a potential drug target, BioEssays 29 (2007) 155–167.
[4] E. Izbicka, R.T. Wheelhouse, E. Raymond, K.K. Davidson, R.A. Lawrence, D. Sun, B.E. Windle, L.H. Hurley, D.D. Von Hoff, Effects of cationic porphyrins as G-quadruplex interactive agents in human tumor cells, Cancer Res. 59 (1999) 639–644.
[5] N.V. Anantha, M. Azam, R.D. Sheardy, Porphyrin binding to quadruplexed T_4G_4, Biochemistry 37 (1998) 2709–2714.
[6] I. Haq, J.O. Trent, B.Z. Chowdhry, T.C. Jenkins, Intercalative G-tetraplex stabilization of telomeric DNA by a cationic Porphyrin, J. Am. Chem. Soc. 121 (1999) 1768–1779.
[7] C. Wei, G. Jia, J. Yuan, Z. Feng, C. Li, A spectroscopic study on the interactions of porphyrin with G-quadruplex DNAs, Biochemistry 45 (2006) 6681–6691.
[8] R.T. Wheelhouse, D. Sun, H. Han, F.X. Han, L.H. Hurley, Cationic porphyrins as telomerase inhibitors: the interaction of tetra-(*N*-methyl-4-pyridyl)porphine with quadruplex DNA, J. Am. Chem. Soc. 120 (1998) 3261–3262.
[9] F.X. Han, R.T. Wheelhouse, L.H. Hurley, Interactions of TMPyP4 and TMPyP2 with quadruplex DNA. Structural basis for the differential effects on telomerase inhibition, J. Am. Chem. Soc. 121 (1999) 3561–3570.
[10] H. Han, D.R. Langley, A. Rangan, L.H. Hurley, Selective interactions of cationic porphyrins with G-quadruplex structures, J. Am. Chem. Soc. 123 (2001) 8902–8913.
[11] G.N. Parkinson, R. Ghosh, S. Neidle, Structural basis for binding of porphyrin to human telomeres, Biochemistry 46 (2007) 2390–2397.
[12] J. Seenisamy, S. Bashyam, V. Gokhale, H. Vankayalapati, D. Sun, A. Siddiqui-Jain, N. Streiner, K. Shin-ya, E. White, W.D. Wilson, L.H. Hurley, Design and synthesis of an expanded porphyrin that has selectivity for the c-MYC G-quadruplex structure, J. Am. Chem. Soc. 127 (2005) 2944–2959.
[13] T. Yamashita, T. Uno, Y. Ishikawa, Stabilization of guanine quadruplex DNA by the binding of porphyrins with cationic side arms, Bioorg. Med. Chem. 13 (2005) 2423–2430.
[14] K. Halder, S. Chowdhury, Quadruplex-coupled kinetics distinguishes ligand binding between G4 DNA motifs, Biochemistry 46 (2007) 14762–14770.
[15] I.M. Dixon, F. Lopez, A.M. Tejera, J.P. Estève, M.A. Blasco, G. Pratviel, B. Meunier, G-quadruplex ligand with 10000-fold selectivity over duplex DNA, J. Am. Chem. Soc. 129 (2007) 1502–1503.
[16] A. Arora, S. Maiti, Effect of loop orientation on quadruplex-TMPyP4 interaction, J. Phys. Chem. B 112 (2008) 8151–8159.
[17] C. Wei, G. Han, G. Jia, J. Zhou, C. Li, Study on the interaction of porphyrin with G-quadruplex DNAs, Biophys. Chem. 137 (2008) 19–23.
[18] C. Wei, G. Jia, J. Zhou, G. Han, C. Li, Evidence for the binding mode of porphyrins with G-quadruplex DNA, Phys. Chem. Chem. Phys. (2009), doi:10.1039/B901027K.
[19] S. Neidle, G.N. Parkinson, The structure of telomeric DNA, Curr. Opin. Struct. Biol. 13 (2003) 275–283.
[20] M.A. Keniry, Quadruplex structures in nucleic acid, Biopolymers 56 (2001) 123–146.
[21] T.A. Gray, K.T. Yue, L.G. Marzilli, Effect of N-alkyl substituents on the DNA binding properties of meso-tetrakis(4-N-alkylpyridinium-4-yl) porphyrins and their nickel derivatives, J. Inorg. Biochem. 41 (1991) 205–219.
[22] J.B. Chaires, Analysis and interpretation of ligand-DNA binding isotherms, Methods Enzymol. 340 (2001) 3–22.
[23] L.R. Keating, V.A. Szalai, Parallel-stranded guanine quadruplex interactions with a copper cationic porphyrin, Biochemistry 43 (2004) 15891–15900.
[24] S. Paramasivan, I. Rujan, P.H. Bolton, Circular dichroism of quadruplex DNAs: applications to structure, cation effects and ligand binding, Methods 43 (2007) 324–331.
[25] M. Lu, Q. Guo, N.R. Kallenbach, Structure and stability of sodium and potassium complexes of dT_4G_4 and dT_4G_4T, Biochemistry 31 (1992) 2455–2459.
[26] J.D. McGhee, P.H. von Hippel, Theoretical aspects of DNA–protein interactions: co-operative and non-co-operative binding of large ligands to a one-dimensional homogeneous lattice, J. Mol. Biol. 86 (1974) 469–489.

[27] R.F. Pasternack, E.J. Gibbs, J.J. Villafranca, Interactions of porphyrins with nucleic acids, Biochemistry 22 (1983) 2406–2414.
[28] T. Lenz, E.Y.M. Bonnist, G. Pljevaljčić, R.K. Neely, D.T.F. Dryden, A.J. Scheidig, A.C. Jones, E. Weinhold, 2-Aminopurine flipped into the active site of the adenine-specific DNA methyltransferase M.TaqI: crystal structures and time-resolved fluorescence, J. Am. Chem. Soc. 129 (2007) 6240–6248.
[29] K. Lang, J. Mosinger, D.M. Wagnerová, Photophysical properties of porphyrinoid sensitizers non-covalently bound to host molecules; models for photodynamic therapy, Coord. Chem. Rev. 248 (2004) 321–350.
[30] A.A. Ghazaryan, Y.B. Dalyan, S.G. Haroutiunian, A. Tikhomirova, N. Taulier, J.W. Wells, T.V. Chalikian, Thermodynamics of interactions of water-soluble porphyrins with RNA duplexes, J. Am. Chem. Soc. 128 (2006) 1914–1921.
[31] J.M. Kelly, M.J. Murphy, D.J. Mcconnell, C.A. Ohuigin, A comparative study of the interaction of 5,10,15,20-tetrakis (N-methylpyridinium-4-yl)porphyrin and its zinc complex with DNA using fluorescence spectroscopy and topoisomerisation, Nucleic Acids Res. 13 (1985) 167–184.
[32] N.N. Kruk, S.I. Shishporenok, A.A. Korotky, V.A. Galievsky, V.S. Chirvony, P.Y. Turpin, Binding of the cationic 5,10,15,20-tetrakis(4-N-methylpyridyl) porphyrin at 5′ CG3′ and 5′GC3′ sequences of hexadeoxyribonucleotides: triplettriplet transient absorption, steady-state and time-resolved fluorescence and resonance Raman studies, J. Photochem. Photobiol. B: Biol. 45 (1998) 67–74.
[33] F.J. Vergeldt, R.B.M. Koehorst, A. van Hoek, T.J. Schaafsma, Intramolecular interactions in the ground and excited states of tetrakis(N-methylpyridyl)porphyrins, J. Phys. Chem. 99 (1995) 4397–4405.
[34] Y. Shen, P. Myslinski, T. Treszczanovicz, Y. Liu, J.A. Koningstein, Picosecond laser-induced fluorescence polarization studies of mitoxantrone and tetrakis porphine/DNA complexes, J. Phys. Chem. 96 (1992) 7782–7787.
[35] K. Zupán, L. Herényi, K. Tóth, Z. Majer, G. Csík, Binding of cationic porphyrin to isolated and encapsidated viral DNA analyzed by comprehensive spectroscopic methods, Biochemistry 43 (2004) 9151–9159.
[36] Y. Liu, J.A. Koningstein, Y. Yevdokimov, Relative cross section and time-resolved fluorescence of porphyrin–DNA complexes, Can. J. Chem. 69 (1991) 1791–1803.
[37] V.S. Chirvony, V.A. Galievsky, N.N. Kruk, B.M. Dzhagarov, P.Y. Turpin, Photophysics of cationic 5,10,15,20-tetrakis-(4-N-methylpyridyl) porphyrin bound to DNA, [poly (dA-dT)]2 and [poly(dG-dC)]2: on a possible charge transfer process between guanine and porphyrin in its excited singlet state, J. Photochem. Photobiol. B: Biol. 40 (1997) 154–162.
[38] K. Phillips, Z. Dauter, A.I. Murchie, D.M. Lilley, B. Luisi, The crystal structure of a parallel-stranded guanine tetraplex at 0.95 Å resolution, J. Mol. Biol. 273 (1997) 171–182.